CARRIER COLLECTION IN THIN-FILM CDTE SOLAR CELLS: THEORY AND EXPERIMENT

A.E. Delahoy, Z. Cheng and K.K. Chin
Department of Physics, Apollo Solar Energy Research Center,
New Jersey Institute of Technology, Newark, NJ 07102, USA
Tel: ++1(973)-642-7553, Fax: ++1(973)-596-5794, e-mail: delahoy@njit.edu

ABSTRACT: The traditional p-n junction theory separates the total solar cell current into a voltage-dependent dark current term and a constant (voltage-independent) light current term. However, thin film CdTe solar cells do not obey the superposition principle. In this work we study the voltage dependence of the collected photocurrent, both theoretically and experimentally. On the modeling side, we develop new equations for calculating the internal quantum efficiency based on a linearly varying electric field in the space charge region. Experimentally, we measure the collected photocurrent resulting from the application of chopped monochromatic light in the presence of a steady white light bias. We show that the minority carrier diffusion length is intensity-dependent, and that it decreases with increasing intensity. This is consistent with the published minority carrier lifetime data measured by time-resolved photoluminescence. We also demonstrate that the minority carrier mobility-lifetime product and the space charge width can be deduced by fitting the predictions of the new collection equations to experimental data taken at two different wavelengths.
Keywords: CdTe, thin film solar cell, modeling

1 INTRODUCTION

Traditional Si p-n junction solar cell theory predicts that the total solar cell current in the light, $J_L(V)$, is

$$J_L(V) = J_D(V) - J_{sc} \quad (1)$$

where the dark current term, $J_D(V)$, is independent of light intensity, and the short-circuit current, J_{sc}, is independent of voltage, i.e. superposition holds. Thin film CdTe solar cells deviate from the superposition model for several reasons. Since a much greater fraction of the light is absorbed in the space charge region (SCR) than in crystalline Si solar cells, and since the diffusion length is short, the photocurrent is dependent on cell voltage via the latter's effect on the width of the SCR, W [1]. Also, a relatively high density of recombination centers in CdTe leads to Shockley-Read-Hall (SRH) recombination in the SCR, and this depends on light intensity and the details of the splitting of the quasi-Fermi levels. If the CdS presents a light-modulated barrier then this can present an additional mechanism for failure of superposition [2]. Failure of superposition is not restricted to polycrystalline thin film cells and has been observed in Si p-n junction cells containing distributed defects.

To develop a replacement for eqn. (1) we observe that, from the continuity equation, and following [3],

$$J_L(V) = q\int_{cell} U(x)dx - q\int_{cell} G(x)dx \quad (2)$$

Superposition can only be valid if the integral of the volume recombination rate $U(x)$ in the light equals the same integral in the dark. In thin film cells, this is generally not true. Based on eqn. (2) we may write

$$J_L(V) = J_{F,L}(V) - J_{ph,L} \quad (3)$$

where $J_{F,L}(V)$ is the forward diode current under illumination (integral of $U(x)$), and $J_{ph,L}$ is the potential photocurrent under illumination (integral of generation rate $G(x)$). Note that, once the solar cell material and structure is defined, we can in principle calculate $J_{F,L}(V)$ through self-consistent solution of Poisson's equation, and the electron and hole continuity equations.

In this paper we analyze the experimental situation in which a steady white bias light (L) is present and a much weaker monochromatic beam (probe beam, p) is superposed. Under this condition, eqn. (3) becomes

$$J_{L+p}(V) = J_{F,L+p}(V) - J_{ph,L} - J_{ph,p} \quad (4)$$

If we separate and shift the recombination loss $R_p(V)$ associated with the probe beam from the diode current to the probe photocurrent term we may write

$$J_{F,L+p}(V) - J_{ph,p} = J_{F,L}(V) + R_p(V) - J_{ph,p}$$
$$= J_{F,L}(V) - \left(J_{ph,p} - R_p(V)\right) = J_{F,L}(V) - J_{ph,p}(V) \quad (5)$$

where $J_{ph,p}(V)$ is now the voltage-dependent photocurrent generated by the probe beam. Subtracting eqn. (3) from eqn. (4) we now have (after making use of (5))

$$J_{L+p}(V) - J_L(V) = J_{ph,p}(V) \quad (6)$$

The LHS is the delta in the measured total cell current, ΔJ_L, due to the probe beam, and we will show with experimental data that the form of ΔJ_L can be written

$$\Delta J_L = J_{ph,p}\eta(V) \quad (7)$$

where $\eta(V)$ is a collection function [4].

This paper provides direct experimental support for eqn. (7). With this in mind, we update previous models for the collection efficiency of minority carriers in n-CdS/p-CdTe junctions (or more generally, one-sided junctions in low lifetime materials). The overall collection efficiency at a given wavelength results from the sum of two processes: a) carrier generation in the SCR, after which a fraction of the minority carriers may be lost to SRH recombination while the remainder are successfully swept out by the electric field and collected; and b) carrier generation in the quasi-neutral region after

which a minority carrier that succeeds in diffusing to the edge of the SCR without recombining may be collected according to process a). Previous models assume a constant electric field in the SCR, while we make the more realistic approximation that the field declines linearly with distance. Finally, we show that basic cell and transport parameters can be deduced using the new collection equations in conjunction with experimental data for $J_{ph}(V)$.

2 EXPERIMENTAL

2.1 Film deposition and cell fabrication

Cadmium telluride solar cells were fabricated in the superstrate configuration with the structure: glass/TCO/n^+-CdS/p-CdTe/graphite/metal back contact. Commercially-available soda-lime glass coated with SnO_2:F/HRT was used as a substrate for the depositions. The CdS (~ 80 nm in thickness) was deposited by chemical bath deposition (CBD) at 88 °C using cadmium chloride, thiourea, ammonium acetate and ammonia, and then annealed at 400 °C. The CdTe (6 - 10 µm in thickness) was deposited by close-spaced sublimation (CSS) at T_s = 600 °C using graphite susceptors and in 10-15 Torr He/O_2 [5, 6]. The CdTe was then soaked in $CdCl_2$/methanol at 80 °C, followed by a furnace anneal under controlled conditions (380 °C, He/O_2, 300 Torr) in order to at improve CdTe structure and minority carrier lifetime. The $CdCl_2$ treatment also appears to promote intermixing of the CdS into the CdTe [7], and the presence of S in the CdTe may serve to passivate defects. To form the back contact, a nitric-phosphoric (NP) acid etch was used to remove the surface oxide, and a very thin layer of Cu was evaporated. A graphite paste containing ZnTe:Cu was applied, followed by annealing in He at 160 °C and then application of a metallic rear electrode. The overall process was similar to that described by Rose et al. [8] and it is also discussed in ref. [9].

2.2 Photocurrent collection measurements

The collection of minority carriers (electrons) in a CdTe solar cell illuminated by monochromatic light was studied by measuring the photocurrent as a function of voltage bias applied to the cell. The cell bias was applied using an op-amp based variable-voltage supply that can source or sink current. The output voltage is held constant regardless of the current. A set of laser diode assemblies having wavelengths of 420, 680, 808, and 850 nm was used to uniformly illuminate the cell. The monochromatic beam was chopped at 133 Hz, while a white LED with reflector was used to provide a steady light bias. The total current from the cell passed through a current-sense resistor in the voltage source thereby providing a voltage signal proportional to the current. To reference this signal to ground it was passed through a unity-gain differential amplifier. The output was fed to a lock-in amplifier whose reading is then proportional to the amplitude of the square-wave photocurrent. The setup proved to be very stable and reproducible, and is shown schematically in Fig. 1.

In this work, the measurements were generally performed under reverse bias, for which the dark current is very small. The purpose of the white light bias is twofold: i) to ensure that the CdS receives above-bandgap light so that it becomes photoconductive (and the risk of it inserting a high resistance is avoided); and ii) to provide a more realistic operating condition in the CdTe as regards carrier generation rate.

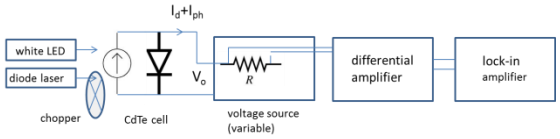

Figure 1: Schematic for photocurrent collection measurements as a function of applied bias using chopped monochromatic light in the presence of a steady white light bias.

3 THEORY

3.1 Background

In the case of thin-film polycrystalline solar cells, the attribution of diode currents to recombination in the SCR was made by Delahoy et al. in the case of $CuInSe_2$[10], and by Phillips et al. for both CIGS and CdTe [11]. Despite the absence of traditional shallow dopants, CdTe can nevertheless be rendered p-type via non-shallow doping [12]. A simplified energy band diagram for the CdS/CdTe solar cell is shown in Fig. 2. While this figure shows E_{Fn} and E_{Fp} to be constant across the SCR, this assumption breaks down under illumination.

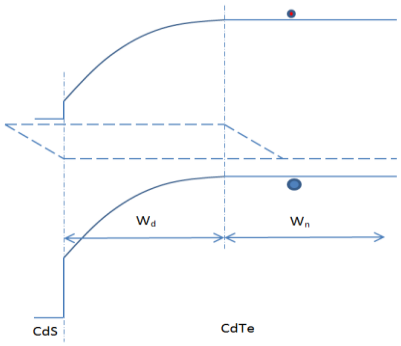

Figure 2: Energy band diagram for CdS/CdTe solar cell (under forward bias but in the dark) showing space charge and neutral regions.

We may calculate the total optical generation rate of carriers $G(x)$ /cm^3/s as a function of depth x in the CdTe by evaluating the generation rate $G(x,\lambda)$ due to a particular wavelength band and summing $G(x,\lambda)$ over all wavelengths of interest:

$$G(x) = \sum_{\lambda} \Phi_{sol}(\lambda)(1-R)e^{-\alpha_{CdS}(\lambda)t}\alpha_{CdTe}(\lambda)e^{-\alpha_{CdTe}(\lambda)x}\Delta\lambda \quad (8)$$

where $\Phi_{sol}(\lambda)$ is the one-sun AM1.5 solar photon flux distribution /cm^2/s/nm, suitably averaged and tabulated for the chosen $\Delta\lambda$, R is the total reflectivity of the CdTe cell from the glass side, $\alpha_{CdS}(\lambda)$ and $\alpha_{CdTe}(\lambda)$ are the optical absorption coefficients of the CdS and the CdTe as a function of wavelength, t is the thickness of the CdS, x is the depth in the CdTe (measured from the CdS/CdTe interface), and $\Delta\lambda$ = 20nm. We used the $\alpha_{CdTe}(\lambda)$ values tabulated in the AMPS software. After calculating $G(x)$ for an appropriate set of x values the total generation rate $G(x)$ can be plotted. Assuming R = 0.1 and t = 100 nm, the result is shown in Fig. 3 below.

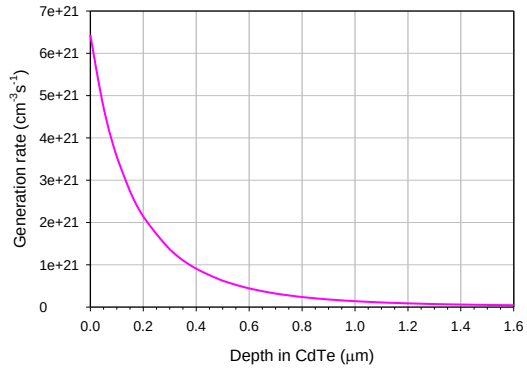

Figure 3: Optical generation rate of carriers as a function of depth in the CdTe.

The potential current density obtainable from a 1.6 μm thick CdTe cell is then just the area under the curve in Fig. 3 x 1E-4 x q, which is 21.4 mA/cm^2 (assuming unity internal quantum efficiency). Of this, 12.3 mA/cm^2 is generated in the first 0.2 μm of the CdTe. This result illustrates one of the advantages of CdTe, namely its very strong optical absorption, and predicts that comparatively poor transport parameters for photogenerated carriers can be tolerated because of the short collection distance.

Previous authors have derived equations for the collected current of minority carriers generated in the SCR and neutral regions of solar cells. This was first done under the assumption of diffusion to the edge of the SCR followed by 100% collection in the SCR [13]. In later work by Debney, for the case of a-Si:H, drift and recombination in the SCR was treated [14]. Kosyachenko considered losses in the SCR through the introduction of both electron and hole drift lengths, thereby arriving at a Hecht-type expression [15]. This approach rejects the minority carrier concept, and we do not consider this a valid model for most CdTe solar cells. We and others [16] previously combined the diffusion and drift processes to yield the total internal quantum efficiency:

$$IQE(\lambda,V) = \frac{\alpha L_d}{1+\alpha L_d}\left[1 - e^{-\frac{W}{L_d}(1+\alpha L_d)}\right] + \frac{\alpha L_n}{1+\alpha L_n} e^{-\frac{W}{L_d}(1+\alpha L_d)} \quad (9)$$

in which L_n and L_d are the electron diffusion length $((kT/q)\,\mu_n\tau_n)^{0.5}$ and drift length $\mu_n\tau_n E$, respectively, and W is the space charge width. Equation (9) is derived under the relatively crude approximation that the electric field E is constant in the SCR (and zero elsewhere).

3.2 New equations based on linear electric field

In contrast to assuming a constant electric field in the space charge region (SCR), we now assume a field $E(x)$ that decreases linearly in the SCR from its value E_0 at the CdS/CdTe interface to zero at $x = W$, the edge of the SCR. This field dependence is identical to that of a one-sided junction with constant doping concentration. Thus, with zero voltage applied to the cell,

$$E(x) = E_0\left(1 - \frac{x}{W}\right); \quad E_0 = 2\frac{V_{bi}}{W}$$

For monochromatic light entering the CdTe, the photon flux N at a depth x is $N(x) = N_0\exp(-\alpha x)$, where $\alpha(\lambda)$ is the optical absorption coefficient of the CdTe at wavelength λ. The carrier generation rate $G(x)$ is therefore

$$G(x) = -\frac{dN}{dx} = \alpha N_0 \exp(-\alpha x)$$

The internal quantum efficiency $IQE_{SCR}(\lambda)$ for minority carriers generated in the space charge region can be written

$$IQE_{SCR}(\lambda) = \frac{1}{N_0}\int_0^W G(x)\eta_{SCR}(x)dx$$

where the collection probability $\eta_{SCR}(x)$ for minority carriers generated at a depth x in the SCR is assumed to be

$$\eta_{SCR}(x) = \exp(-\frac{t}{\tau})$$

where τ is the minority carrier lifetime and t (implicitly a function of x) is the time spent in the SCR. Since the drift velocity dx/dt of the minority carriers is $\mu E(x)$, we may calculate the time spent in the SCR as

$$t = \int_0^x \frac{dx}{\mu E_0(1-\frac{x}{W})} = -\frac{W}{\mu E_0}\ln(1-\frac{x}{W})$$

Hence,

$$IQE_{SCR}(\lambda) = \int_0^W \alpha\exp(-\alpha x)\exp\left(\frac{W}{\mu\tau E_0}\ln\left(1-\frac{x}{W}\right)\right)dx$$

$$i.e.\ IQE_{SCR}(\lambda) = \int_0^W \alpha\exp(-\alpha x)\left(1-\frac{x}{W}\right)^a dx \quad (10)$$

where the exponent a (generally <<1) is

$$a = \frac{W}{\mu\tau E_0} = \frac{W}{L_{d0}} \quad (11)$$

As will be seen shortly, we will restrict the drift region to $0 < x < x_1$, where x_1 is slightly smaller than W, rather than $0 < x < W$. The integral can in principle be expressed in terms of the incomplete Gamma function $\Gamma(a, x)$. However, it is straightforward to evaluate the integral numerically, and that was the method used for the calculations in this paper.

We may calculate the internal quantum efficiency for minority carriers generated in the neutral region, IQE_{neut}, by first calculating the probability that a carrier diffuses to the edge of the SCR, and multiplying by the probability of collection in the SCR. To avoid infinite collection times for carriers at $x = W$, we set the demarcation depth for changeover from diffusion to drift at the depth x_1 (< W) for which the minority carrier diffusion length L_n equals the minority carrier drift length L_d. This is illustrated in Fig. 3. Thus, with $E(x_1) = E_1$, we set

$$L_n = \sqrt{\frac{kT}{q}\mu\tau} = L_d = \mu\tau E_1$$

$$E_1 = \sqrt{\frac{kT}{q}\frac{1}{\mu\tau}}; \quad x_1 = \left(1-\frac{E_1}{E_0}\right)W$$

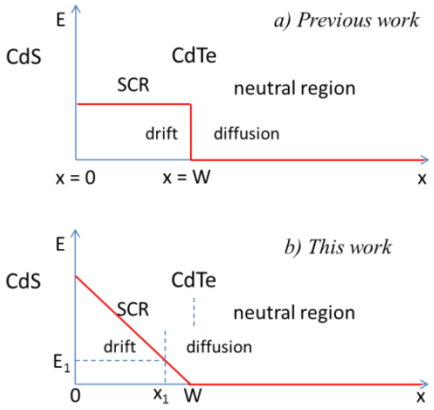

Figure 3: Electric field versus distance and demarcation between regions of minority carrier drift and diffusion for: a) previous work (constant field in SCR and demarcation at $x = W$); and b) this work (linear field in SCR and demarcation at $x = x_1$ with field E_1).

With a new coordinate system having $x = 0$ at a depth x_1 in the SCR, $\eta_{neut}(x)$, the probability that a minority carrier generated in the neutral region at depth x diffuses to $x = 0$ (the point at which drift takes over), is

$$\eta_{neut}(x) = \exp(-\frac{x}{L_n})$$

This analysis assumes that the thickness of the cell >> L_n. We therefore have

$$IQE_{neut}(\lambda) = \int_0^{\infty} \alpha \exp\{-\alpha(x_1 + x)\} \exp(-\frac{x}{L_n}) \left(1 - \frac{x_1}{W}\right)^a dx$$

yielding

$$IQE_{neut}(\lambda) = \frac{\alpha L_n}{1 + \alpha L_n} \exp(-\alpha x_1) \left(1 - \frac{x_1}{W}\right)^a \quad (12)$$

If there is a non-zero recombination velocity S at the CdS/CdTe interface, then we may introduce the field-dependent, but wavelength-independent, collection parameter β_i (< 1) representing recombination at this interface, where [17],

$$\beta_i = \frac{1}{1 + \frac{S}{\mu_n E}}$$

The final expression for the external quantum efficiency $QE(\lambda)$ is then

$$QE(\lambda) = (1 - R) \exp(-\alpha_{CdS} t_{CdS}) \beta_i \{IQE_{drift}(\lambda) + IQE_{neut}(\lambda)\} \quad (13)$$

where

$$IQE_{drift}(\lambda) = \int_0^{x_1} \alpha \exp(-\alpha x) \left(1 - \frac{x}{W}\right)^a dx \quad (14)$$

and the limits of integration are now 0 and x_1.

When a voltage V is applied to the cell, the built-in voltage is reduced (for $V > 0$) from V_{bi} to $V_{bi} - V$. Also, since the zero-bias width of the SCR is

$$W_0 = \sqrt{\frac{2\epsilon V_{bi}}{qN_a^-}}$$

both the depletion width and peak electric field become functions of V

$$W(V) = \sqrt{\frac{2\epsilon(V_{bi} - V)}{qN_a^-}} = W_0 \sqrt{1 - \frac{V}{V_{bi}}}$$

$$E_0(V) = \frac{2(V_{bi} - V)}{W} = E_0 \sqrt{1 - \frac{V}{V_{bi}}}$$

The dependence of the electric field on both V and x becomes

$$E(V, x) = E_0 \sqrt{1 - \frac{V}{V_{bi}}} \left(1 - \frac{x}{W_0 \sqrt{1 - \frac{V}{V_{bi}}}}\right)$$

On the other hand, the exponent a becomes

$$a = \frac{W(V)}{\mu\tau E_0(V)} = \frac{W_0}{\mu\tau E_0} \quad (15)$$

and is hence independent of V.

To illustrate the use of the equations derived above (linear field case) we have calculated the external quantum efficiency $QE(\lambda, 0)$ at zero bias for a CdS/CdTe solar cell for a particular set of parameters and show the result in Fig. 4 below. For the parameters stated in the figure and caption, J_{sc} under AM1.5 1000 W/m^2 irradiance is 20.1 mA/cm^2. The figure also shows the decomposition of $QE(\lambda)$ into contributions from the drift and diffusion regions (18.5 mA/cm^2 and 1.6 mA/cm^2).

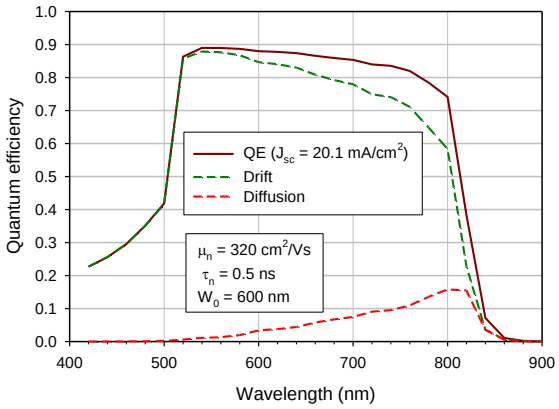

Figure 4: Modeled external quantum efficiency (at zero bias) versus wavelength assuming $R = 0.1$, $t_{CdS} = 0.1$ µm, $V_{bi} = 1.0$ V, $S = 20000$ cm/s and critical transport and junction parameters as stated in the figure. The modeling used the linear field equations derived in the text.

4 EXPERIMENTAL RESULTS AND ANALYSIS

The results for photocurrent collection in a CdS/CdTe cell of middling performance (FF ≈ 0.6) are shown in Fig. 5 as a function of cell bias (i.e. $J_{ph}(V)$) for three different wavelengths of incident light. The data show that the photocurrent for very strongly absorbed blue light saturates under reverse bias, while at longer wavelengths the recombination losses are greater because of the greater drift and diffusion distances, but can be reduced by increasing the drift field and the width of the space charge region through application of reverse bias.

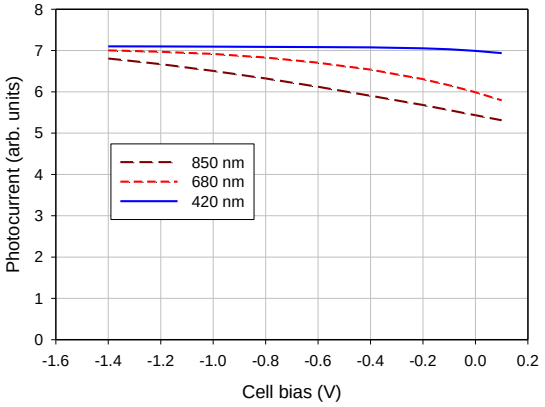

Figure 5: Collection of chopped photocurrent as a function of cell bias in the presence of 0.03 suns white light bias.

Thus, the photocurrent J_{ph} can be fully (or almost fully) collected under sufficient reverse bias, so that we can write

$$J_{ph}(V) = J_{ph}\eta(V) \qquad (16)$$

where $\eta(V)$ is a collection function that tends to unity under reverse bias and is < 1 otherwise [4]. We can find $\eta(V)$ from experimental data via eqn. (16), or with the notation of the Introduction

$$\eta(V) = \frac{\Delta J_L}{J_{ph,p}} \qquad (17)$$

The general behavior of these experimental results are well accounted for by both the constant field and linear field *IQE* equations ((9), and (12) + (14)). From the full saturation of J_{ph}(420 nm, V) under reverse bias we conclude that the interfacial collection parameter β is >0.99 for all CdS/CdTe cells fabricated as described above. The photocurrent curves can also be measured under forward bias for different wavelengths of the incident light. In this case the curve shape at each wavelength becomes indicative of the cell fill factor for this wavelength of light.

For incident monochromatic light close to the band edge of CdTe that is only very weakly absorbed we have shown that eqn. (9) reduces to

$$IQE(\lambda, V) = \frac{\alpha}{1+\alpha L_n}[W(V) + \beta L_n] \qquad (18)$$

where $\beta = 1 - W_0/L_{d0}$ (Note that β is close to unity). Hence a plot of $IQE(W)$, or equivalently J_{ph}, versus W should be a straight line whose intercept on the W axis is βL_n (in units of W_0), where L_n is the minority carrier diffusion length. (We believe that the weak absorption limit (eqn. (18)) is also predicted by the linear field equations.) Using an 850 nm laser diode as a light source, and the setup of Fig. 1, the photocurrent was measured as a function of voltage bias for five different intensities of white light bias. All five plots of J_{ph} versus W were surprisingly linear; for clarity, only three sets of data are shown in Fig. 6. The intercepts for all five light levels are shown in Table I. It can be seen that only a little light is sufficient to make a jump in βL_n, after which βL_n peaks and then declines with increasing intensity.

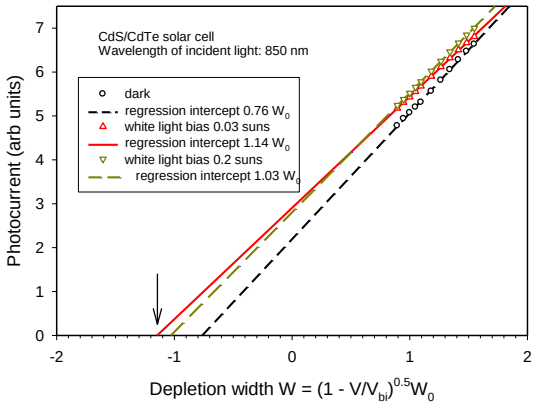

Figure 6: Plot of photocurrent (proportional to $IQE(V)$) for weakly absorbed light as a function of depletion width and hence estimation of the minority carrier diffusion length in p-CdTe.

This results from the increased splitting of the electron and hole quasi-Fermi levels. We conclude that the minority carrier lifetime resulting from SRH recombination in CdTe is intensity-dependent and decreases with increasing intensity. This is consistent with the published minority carrier lifetime data measured by time-resolved photoluminescence [18], but is believed to be the first time this has been demonstrated through collection measurements.

Table I: Dependence of minority carrier diffusion length on light intensity.

Light bias (suns)	βL_n
0	0.76
0.005	1.10
0.030	1.14
0.076	1.11
0.20	1.03

We further observe that the *IQE* equations make very definite predictions for *QE* ratios at different cell biases depending on the input parameters μ_n, τ_n, and W_0. Since μ_n and τ_n enter into the collection equations only as their product, there are essentially only two parameters ($\mu_n\tau_n$ and W_0) to be fitted. In this paper we have chosen to analyze the two ratios QE(-1.4V)/QE(-0.8V) at the wavelengths 680 nm and 850 nm for the fitting procedure. The QE values were modeled using the linear field equations (12) – (14). Good agreement between the modeled and experimental ratios was obtained for $\mu_n\tau_n$ = 5.1 x 10^{-8} cm^2/V and W_0 = 3.0 x 10^{-5} cm, as shown in Table II.

Table II: Adjustment of $\mu_n\tau_n$ and W_0 to bring the modeled and experimental values of the ratios QE(-1.4V)/QE(-0.8V) into agreement. The fitted parameters are $\mu_n\tau_n$ = 5.1 x 10^{-8} cm^2/V and W_0 = 3.0 x 10^{-5} cm.

Quantity	680 nm		850 nm	
	theory	expt.	theory	expt.
QE(-0.8V) or J_{ph}	0.8006	4.992	0.0453	6.322
QE(-1.4V) or J_{ph}	0.8195	4.869	0.0489	6.806
QE(-1.4V)/ QE(-0.8V)	1.024	1.025	1.079	1.077

We may remark that the importance of the $\mu_n\tau_n$ product reveals that improvement of the electron mobility in thin-film CdTe, and not just the lifetime, is important for CdTe solar cell performance.

5 DISCUSSION

The length scales in this problem are set by the depletion width, the drift lengths, and the inverse of the optical absorption coefficient for a given wavelength of illumination. It is known that the CdS/CdTe interface is to some extent intermixed so that the near-surface absorber layer is an alloy $CdTe_{1-x}S_x$. The bandgap of this alloy has a minimum (≈ 1.4 eV) for x around 0.25-0.30 [7, 19]. We recognize that the modified optical properties of this material should be taken into account in calculating the carrier generation profile. Although the effective bandgap of the absorber is reduced, it remains unclear whether the device is a heterojunction or a buried homojunction.

The modelling has been conducted assuming a plane junction and a one-dimensional spatial coordinate. However, if potential barriers at the CdTe grain boundaries [20] repel carriers of one type (e.g. holes) then electron collection might also take place sideways.

Another assumption that this work has implicitly made is that the minority carrier lifetime τ_n is position-independent. Other aspects of our work have shown that this is not the case [21, 22]. Whether collection equations involving different τ_n in the neutral and SCR regions can give a better cell description remains to be seen. The alternative is a full numerical simulation of the cell.

In future work we plan to examine cells with higher fill factor, and to make more extensive correlations between collection, J-V, QE, and C(V) measurements. There also exists the opportunity to determine the temperature dependence of $\mu_n\tau_n$.

6 CONCLUSIONS

The collection of minority carriers in p-type CdTe solar cells has been studied both theoretically and experimentally. Assuming for the first time a linear electric field in the space charge region, new equations have been written for collection via drift in the space charge region and by diffusion in the neutral region to a plane at which drift becomes dominant. The interpretation of the change in total cell current with intensity as a voltage-dependent photocurrent was also clarified. Photocurrent collection experiments as a function of applied voltage using weakly absorbed light and various levels of white light bias have shown that the minority carrier diffusion length is intensity dependent. Collection data obtained at two different wavelengths and voltages proved sufficient to deduce the $\mu_n\tau_n$ product and space charge width W_0 by fitting to the predictions of the equations derived for *IQE* under the linear field assumption. The above results, namely the dependence of collection efficiency on voltage and the dependence of lifetime on intensity, account for some of the differences in behavior between CdTe solar cells and crystalline Si solar cells.

ACKNOWLEDGEMENTS

The authors would like to acknowledge Apollo Solar Energy, Inc. for early support of this work. In addition, the authors thank Mr. G. Liu for CdS depositions and Mr. Z. Wang for useful discussions.

REFERENCES

[1] X. Liu, J. Sites, J. Appl. Phys., 75 (1994) 577.
[2] G. Agostinelli, E.D. Dunlop, D.L. Bätzner, A.N. Tiwari, P. Nollet, M. Burgelman, and M. Köntges, Proc. 3rd World Conf. on Photovoltaic Energy Conversion (2003) 356.
[3] F.A. Lindholm, J.G. Fossum, E.L. Burgess, IEEE Trans. Electron Devices, ED-26 (1979) 165.
[4] S. Hegedus, D. Desai, C. Thompson, Prog. Photovolt: Res. Appl. 15 (2007) 587.
[5] T.C. Anthony, A.L. Fahrenbruch, and R.H. Bube, J. Vac. Sci. Technol. A2 (1984) 1296.
[6] T.L. Chu, S.S. Chu, and S.T. Ang, J. Appl. Phys. 64 (1988) 1233.
[7] B.E. McCandless, K.D. Dobson, Solar Energy 77 (2004) 839.
[8] D.H. Rose, F.S. Hasoon, R.G. Dhere , D.S. Albin, R.M. Ribelin, X.S. Li, Y. Mahathongdy, T.A. Gessert and P. Sheldon, Prog. Photovolt: Res. Appl. 7 (1999) 331.
[9] P. Kharangarh, D. Misra, G.E. Georgiou, A.E. Delahoy, Z. Cheng, G. Liu, H. Opyrchal, T. Gessert and K. K. Chin, 38th IEEE PVSC, 2012.
[10] A.E. Delahoy, F. Faras, A. Sizemore, F. Ziobro, and Z. Kiss, AIP Conf. Proc. Vol. 268, (AIP, New York, 1992; Editor: Rommel Noufi) 170.
[11] J.E. Phillips, R.W. Birkmire, B.E. McCandless, P.V. Meyers, and W.N. Shafarman, phys. stat. sol. (b) 194 (1996) 31.
[12] J. Ma, S-H. Wei, T.A. Gessert, K.K. Chin, Phys. Rev. B 83 (2011) 245207.
[13] W.W. Gärtner, Phys. Rev. 116 (1959) 84.
[14] B.T. Debney, Proc. 1st European Photovoltaic Solar Energy Conference, (1977) 216; and Solid State and Electron Devices 2 (1978) S15.
[15] L.A. Kosyachenko, E.V. Grushko, V.V. Motushchuk, Sol. Energy Mater. Sol. Cells 90 (2006) 2201.
[16] M. Hädrich, H. Metzner, U. Reislöhner, C.Kraft, Sol. Energy Mater. Sol. Cells 95 (2011) 887.
[17] K.W. Mitchell, A.L. Fahrenbruch, R.H. Bube, J. Appl. Phys. 48 (1977) 4365.
[18] W. K. Metzger, D. Albin, D. Levi, P. Sheldon, X. Li, B. M. Keyes, and R. K. Ahrenkiel, J. Appl. Phys., 94, (2003) 3549.
[19] B.E. McCandless and J.R. Sites, Chapter 14 in *Handbook of Photovoltaic Science and Engineering* 2nd edition, edited by A. Luque and S. Hegedus, Wiley, Chichester (2011) 600.
[20] K. Durose, D. Boyle, A. Abken, C.J. Ottley, P. Nollet, S. Degrave, M. Burgelman, R. Wendt, J. Beier, D. Bonnet, phys. stat. sol. (b) 229 (2002) 1055.
[21] K.K. Chin J. Appl. Phys. 111 (2012) 104509.
[22] Z. Cheng, Z. Su, Z. Wang, A.E. Delahoy, K.K. Chin, to be published.